

# Ambipolar diffusion length and photoconductivity measurements on “midgap” hydrogenated microcrystalline silicon

M. Goerlitzer,<sup>a)</sup> N. Beck, P. Torres, J. Meier, N. Wyrsh, and A. Shah  
*Institut de Microtechnique, Université de Neuchâtel, CH-2000 Neuchâtel, Switzerland*

Hydrogenated microcrystalline silicon ( $\mu c$ -Si:H) deposited by VHF plasma-enhanced chemical vapor deposition has recently been proven to be fully stable, with respect to light-induced degradation, when adequately used in  $p$ - $i$ - $n$  solar cells. Stable solar cells efficiencies of 7.7% have been obtained with single-junction cells, using “midgap” microcrystalline  $i$ -layers, having an optical gap of around 1 eV. In the present paper, the electronic transport properties of such microcrystalline layers are determined, by the steady-state photocarrier grating method (SSPG) and steady-state photoconductivity measurements, in a coplanar configuration. The conditions for the validity of the procedure for determining the ambipolar diffusion length,  $L_{amb}$ , from SSPG measurements (as previously theoretically derived in the context of amorphous silicon) are carefully re-examined and found to hold in these  $\mu c$ -Si:H layers, taking certain additional precautions. Otherwise, e.g., the prevalence of the “lifetime” regime (as opposed to the “relaxation time” regime) becomes questionable, in sharp contrast with the case of amorphous semiconductors, where this condition is almost never a problem. For the best layers measured so far,  $L_{amb}$  is about twice as high and the photoconductivity  $\sigma_{photo}$  four times as high in  $\mu c$ -Si:H, when compared to device quality  $a$ -Si:H. Until now, the highest values of  $L_{amb}$  found by the authors for  $\mu c$ -Si:H layers are around  $3 \times 10^{-5}$  cm.

## INTRODUCTION

Hydrogenated microcrystalline silicon ( $\mu c$ -Si:H) has recently been very successfully incorporated as a photovoltaically active  $i$ -layer in solar cells.<sup>1,2</sup> This success raises the question of measuring both electronic and optical properties of this promising new material. The optical properties have already partially been studied,<sup>1,3</sup> but to the best of our knowledge the electronic transport properties under illumination have so far not been systematically investigated.<sup>4,5</sup> The aim of this paper is to study the electronic transport properties in “midgap” (Fermi level near midgap) microcrystalline silicon in coplanar configuration. For this purpose we used the following two methods, steady-state photocarrier grating (SSPG)<sup>6,7</sup> and steady-state photoconductivity (SSPC), which are well established for amorphous silicon ( $a$ -Si:H).

In the SSPG technique, one measures the small-signal photocurrent perpendicular to optical fringes created by the interference of two laser beams. These fringes generate a spatially nonuniform carrier density in the sample; thus, the conductivity of the latter depends on the ratio between the grating spacing ( $\Lambda$ ) and the ambipolar diffusion length ( $L_{amb}$ ): when the grating spacing is much longer than the carrier diffusion length, a well-defined concentration grating of photocarriers is created in the sample; on the other hand, when the grating spacing is comparable to or shorter than the diffusion length, this concentration grating is “blurred” and an almost uniform carrier concentration is formed. The coplanar photocurrent is measured, both when the two light beams are coherent ( $J_{par}$ ) and when they are non coherent ( $J_{perp}$ ): one measures the changes in the photoconductivity between the two configurations, for different grating spacing.

The variation of  $\beta = J_{par}/J_{perp}$  with  $\Lambda$  allows one to relate analytically the experimental data to the ambipolar diffusion length.<sup>7</sup>

SSPC gives directly the photoconductivity, which can be expressed as:<sup>8</sup>

$$\sigma_{photo} = e \mu_n^0 n_f + e \mu_p^0 p_f, \quad (1)$$

( $e$  the elementary charge,  $\mu_{n,p}^0$  the mobilities of free electrons, free holes respectively and  $n_f, p_f$  the free carriers densities) with the sole assumption of using the model of transport by free carriers above the mobility edge. On the other hand, SSPG poses more problems while trying to extract the diffusion length from  $\beta$ , as all the following conditions have to be fulfilled: (1) the existence of two distinct characteristic lengths, identifiable as the ambipolar diffusion length ( $L_{amb}$ ) and the dielectric relaxation length ( $L_{diel}$ ), (2) diffusion prevails over drift, and (3) the dielectric relaxation length is short enough to ensure the quasineutrality in the transport region. These conditions are conditions on the material itself; an additional experimental condition (4) is necessary: the grating spacing has to be of the same order as the diffusion length. Assuming the Einstein equations, postulating a given density of localized gap states (no explicit form is needed) and observing that it generally exists a power-law dependency for photoconductivity as a function of the generation ( $\sigma_{photo} \propto G^\gamma$ ) the following equation is deduced:<sup>7</sup>

$$\beta = 1 - [2\phi / (1 + 4\pi^2 L_{amb}^2 / \Lambda^2)]^2, \quad (2)$$

where  $\phi = \gamma^2 \gamma_0$ , with  $\gamma_0$  an optical grating quality factor. Thus, a plot of  $1/\Lambda^2$  vs  $\sqrt{2/(1-\beta)}$  (so-called “Balberg plot”) should give a straight line and any deviation from such a straight line raises doubts on the validity of the measurements. However, the observation of a straight line is in-

<sup>a)</sup>Electronic mail: goerlitzer@imt.unine.ch

sufficient to positively confirm that the measured length is the ambipolar diffusion length. As a check, one has actually to ensure that this length does not vary strongly with increasing illumination intensity, like the dielectric relaxation length would do<sup>9</sup> ( $L_{\text{diel}}^2 \propto \epsilon/\sigma_{\text{photo}}$ , with  $\epsilon$  the dielectric constant of the material).

Thus far, the only model required is a power law for the photoconductivity. If, for  $\mu c$ -Si:H we observe this power law, the SSPG technique (with its small signal approach) can be considered an appropriate method for the evaluation of the ambipolar diffusion length, assuming a measured variation of  $\beta$  as given by Eq. (2) and the above conditions are fulfilled.

In addition, we can evaluate for  $\mu c$ -Si:H, also, the parameter  $b$ ,<sup>10</sup> a parameter that reflects the position of the two quasi-Fermi-levels with respect to midgap.<sup>11</sup> Introducing the general recombination times  $\tau_n^R$  for electrons and  $\tau_p^R$  for holes, which basically take into account all recombination processes via all available recombinations centers, we have

$$\sigma_{\text{photo}} = eG(\mu_n^0 \tau_n^R + \mu_p^0 \tau_p^R), \quad (3)$$

and

$$L_{\text{amb}}^2 = \frac{kT}{e} \frac{\mu_n^0 \tau_n^R \mu_p^0 \tau_p^R}{\mu_n^0 \tau_n^R + \mu_p^0 \tau_p^R} C, \quad (4)$$

with  $C$  a constant between 1 and 2,<sup>12</sup>  $k$  the Boltzmann constant, and  $T$  the temperature. In the case of an observed power law for the square of the ambipolar length  $L^2 \propto G^\lambda$ ,  $C$  becomes  $C = 1 + \lambda + \gamma$ .

$b$  can be expressed as a function of the photoconductivity and the diffusion length with Eq. (3) and (4):

$$\frac{b}{(b+1)^2} = \frac{L_{\text{amb}}^2 e^2 G}{kT \sigma_{\text{photo}} C}. \quad (5)$$

We have to emphasize here that no particular model of recombination has been introduced to evaluate Eqs. (3)–(5), so we can evaluate  $L_{\text{amb}}$ ,  $\sigma_{\text{photo}}$ , and  $b$  for  $\mu c$ -Si:H without any further restrictions, except those mentioned at the beginning.

## EXPERIMENT

The films studied in this paper were deposited by the VHF-GD deposition technique (70–130 MHz)<sup>13</sup> under various conditions. In order to study nearly intrinsic microcrystalline layers (with the Fermi level near midgap, since deposited microcrystalline silicon is usually an  $n$ -type material), some samples were prepared by adding small traces of diborane<sup>14</sup> while the others were prepared with our new deposition method using a gas purifier.<sup>15</sup> One series was also deposited using various dilutions of silane in hydrogen, to study the transition between  $\mu c$ -Si:H and  $a$ -Si:H. All films were deposited on AF45 (Schott) glass substrates at deposition set point temperature of 250 °C (calculated effective temperature: 220 °C) and with thicknesses between 1.5 and 3.1  $\mu\text{m}$ . The measurements were done with coplanar aluminum contacts (gap of 0.5 mm) using a krypton laser (wavelength 647 nm). All samples were annealed at 180 °C, and their light-induced degradation behavior at 647 nm for an intensity of 200 mW/cm<sup>2</sup> (generation rate of around  $2 \times 10^{21}$

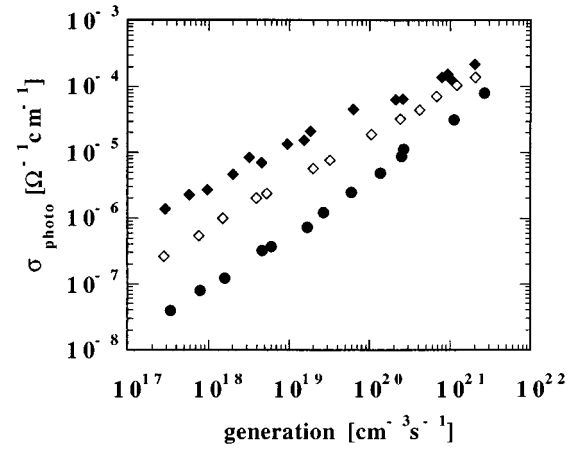


FIG. 1. Typical power law behavior for the photoconductivity as a function of generation rate for our microcrystalline silicon samples.

$\text{cm}^{-3} \text{s}^{-1}$ ) was checked for at least 30 min. No observable degradation in the photoconductivity has been observed in the microcrystalline samples, except for the samples with the two higher dilution ratios (7.6% and 10% of  $\text{SiH}_4$  in  $\text{H}_2$ ), which have amorphous behavior with respect to optical absorption and degraded. For this reason the measurements for these two samples were performed with generation rate less than  $10^{20} \text{ cm}^{-3} \text{ s}^{-1}$ .

## GENERAL OBSERVATIONS

The first observation we make about our microcrystalline samples is their power law dependency of photoconductivity as a function of generation rate (Fig. 1).

The second observation is their large, room-temperature dark conductivity ( $\sigma_{\text{dark}}$ ) compared to  $a$ -Si:H. That renders the evaluation of SSPG more difficult by reducing the variation of  $\beta$  with the change of the grating spacing (Fig. 2): the measurement becomes less sensitive and more difficult to perform, but it still delivers correct results.<sup>7</sup> Eq. (2) becomes:

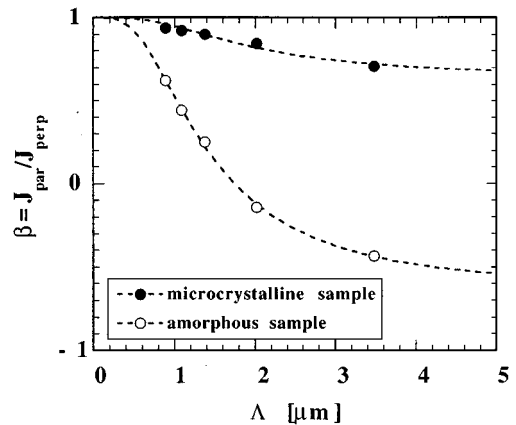


FIG. 2. Typical variation of  $\beta$  as a function of the grating spacing for a microcrystalline silicon sample, and as a comparison, for an amorphous silicon sample (generation of  $3.9 \times 10^{20} \text{ s}^{-1} \text{ cm}^{-3}$ ). The dashed lines are fits to Eq. (6).

$$\beta = 1 - [2\phi\gamma_d / (1 + 4\pi^2 L_{amb}^2 / \Lambda^2)^2], \quad (6)$$

with the reducing factor

$$\gamma_d = \sigma_{photo} / (\sigma_{photo} + \sigma_{dark}). \quad (7)$$

This low sensitivity implies that for some samples, a rather high generation rate has to be used, in order to limit the error in the measurements.

Unfortunately, the measurements of  $\beta(\Lambda)$  for  $\mu c$ -Si:H samples show some deviation from the predicted behavior, i.e., from a straight line in the Balberg plot, and this for small grating spacings (shorter than  $2 \mu\text{m}$ ) and for low illumination intensities (no typical value can be given, as they differ from sample to sample). So, some further observations and discussions are needed to correctly evaluate the diffusion length.

Some possibilities that could basically be cited as reasons for this deviation can easily be ruled out by simple measurements. The hypothesis that the drift is overriding diffusion transport can be excluded because  $\beta$  does not change with a variation of the applied voltage used for the measurement.<sup>12</sup> No heating of the sample from the illumination with the laser light can be invoked, since cooling the sample with air does not change the measurements. Finally, optical scattering can also be ruled out: it has already been observed in  $a$ -Si:H,<sup>3</sup> and measurement of the scattered reflection vs the specular reflection indicates the existence of optical scattering in our samples (for a wavelength of 647 nm). However, the speculation that the small grating spacings are “blurred” due to optical scattering has not been verified (no optical cancellation of the fringes is observed after their passage through the sample).

If surface recombination is present, a nonuniform generation can also lead to a somewhat different behavior for the small gratings. The variation of  $\beta$  in this case becomes:<sup>16</sup>

$$\beta = 1 - [2\phi / (1 + 4\pi^2 L_{amb}^2 / \Lambda^2)^2] g_s^2(\Lambda), \quad (8)$$

with  $g_s^2(\Lambda)$  the correction factor due to the surface recombination velocity. Because  $g_s$  depends on  $\Lambda$ , and is equal or bigger than unity, the Balberg plot is no longer a straight line, but varies less at large  $\Lambda$  than at small  $\Lambda$ . This agrees with our observations (Fig. 3); but, as the optical absorption of our samples is typically around  $1 \times 10^4 \text{ cm}^{-1}$ , a uniform generation can be assumed for our thicknesses and this hypothesis can again be ruled out. In addition, the ambipolar diffusion length can be deduced even if surface recombination is prevalent by carrying out the SSPG measurement for gratings where straight lines are available.

Another possibility is that the condition of an ambipolar length bigger than the dielectric length is not fulfilled. It has been demonstrated that the presence of non-negligible space charge in the layer under test leads to a concave curve for the “Balberg plot.”<sup>17</sup> Increasing the illumination intensity decreases  $L_{diel}$ , and the sample moves towards a regime governed by ambipolar diffusion. We observe that, with increasing intensity, the curve in the Balberg plot tends to become a straight line (see again Fig. 3). Furthermore,  $L_{amb}^2$  (evaluated in the regions where straight lines are available) does not vary strongly with light intensity (see Fig. 4). The dominance

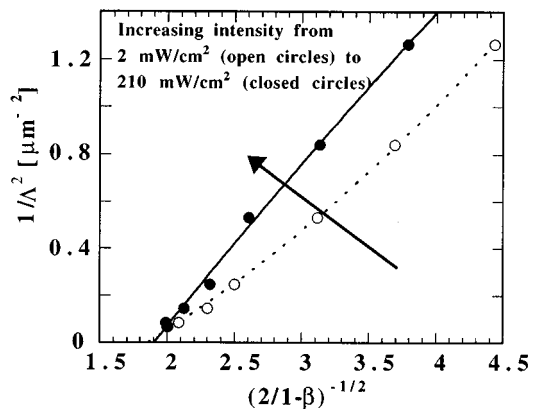


FIG. 3. Typical variation of the curve in the Balberg plot for the SSPG evaluation, where the slope is smaller for large values of  $\Lambda$  than for small values of  $\Lambda$  (open circles). This situation can be expected when surface recombination is prevalent or when the SSPG conditions are not fulfilled (concave curve). Increasing the illumination intensity leads to a straight line in the Balberg plot (closed circles).

of dielectric effects would have given a strong variation of the measured length, as  $L_{diel}$  is approximately inversely proportional to the photoconductivity. As a consequence, we can interpret the measured length as the ambipolar diffusion length. Note that the power law dependency of  $L_{amb}^2$  as a function of the generation seen on Fig. 4 allows the evaluation of the midgap character of the samples with the parameter  $b$ .

## RESULTS AND DISCUSSION

As already stated, the photoconductivity, as well as the ambipolar length of  $\mu c$ -Si:H, shows power law dependency as a function of the generation rate.

The values obtained for the photoconductivity and the ambipolar diffusion length as a function of the Fermi level of the sample, monitored by the parameter  $b$ , are shown in Fig. 5. The material is considered midgap if  $b \approx 50$ ,<sup>18</sup> so most of our samples are clearly midgap. The values for  $L_{amb}$  and

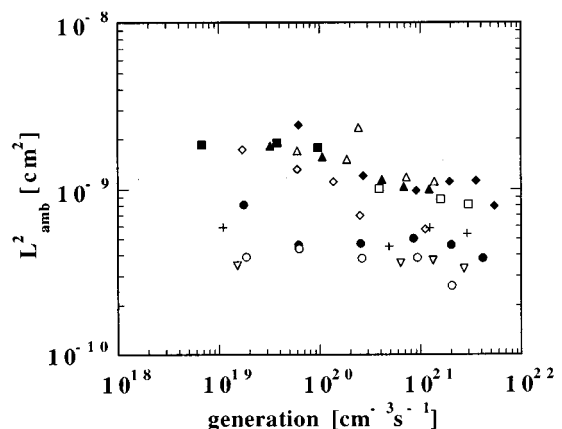


FIG. 4. Variation of the square of the ambipolar diffusion length  $L_{amb}$  as a function of increasing generation for hydrogenated microcrystalline silicon  $\mu c$ -Si:H.

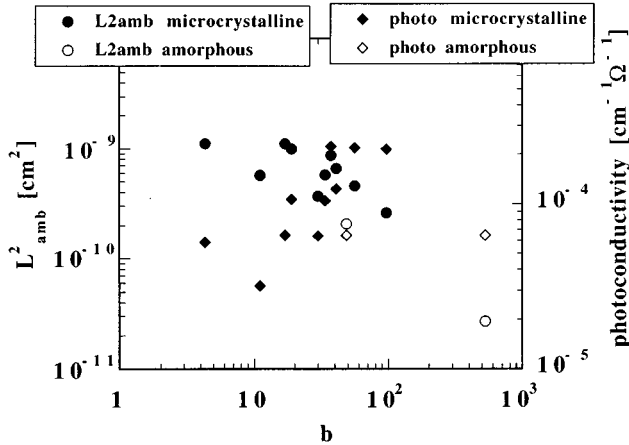


FIG. 5. Ambipolar diffusion length  $L_{\text{amb}}$  and photoconductivity  $\sigma_{\text{photo}}$  as a function of  $b$  for a generation around  $1.5 \times 10^{21} \text{ cm}^{-3} \text{ s}^{-1}$ . The values for the amorphous samples (obtained at high hydrogen dilution) are extrapolated from low generations with the power laws we found.

$\sigma_{\text{photo}}$  are comparable or higher for  $\mu c\text{-Si:H}$  than for  $a\text{-Si:H}$ , for a generation rate around  $1.5 \times 10^{21} \text{ cm}^{-3} \text{ s}^{-1}$ .

The power law exponents observed for the photoconductivity, the square of the ambipolar diffusion length, and  $b$  as a function of the generation rate for midgap  $\mu c\text{-Si:H}$  are similar to those for undoped, amorphous silicon (see Table I). The power law exponent of  $b$  is always negative in our  $\mu c\text{-Si:H}$  samples. In amorphous silicon it is generally positive, but some negative values have also been measured (note that only one sample has a  $\gamma$  with a value of 0.5; the others have values higher than 0.6).

The parameter  $b$  correlates well with the measured dark conductivity activation energy (Fig. 6). We have thereby evaluated the activation energy by fitting the activated dark conductivity according to the well-known equation:

$$\sigma_{\text{dark}} = \sigma_0 \exp\left(-\frac{E_{\text{act}}}{kT}\right), \quad (9)$$

near the room temperature, with  $\sigma_0$  and  $E_{\text{act}}$  as fitting parameter.

The observations made for our  $\mu c\text{-Si:H}$  are quite surprising: even if in our samples the amorphous volume fraction is generally very small,<sup>19</sup> the materials studied here show similar behavior as undoped amorphous silicon, but the values obtain for  $\sigma_{\text{photo}}$  and  $L_{\text{amb}}$  are enhanced.

To check the importance of the amorphous volume fraction, a series with various hydrogen dilutions has also been

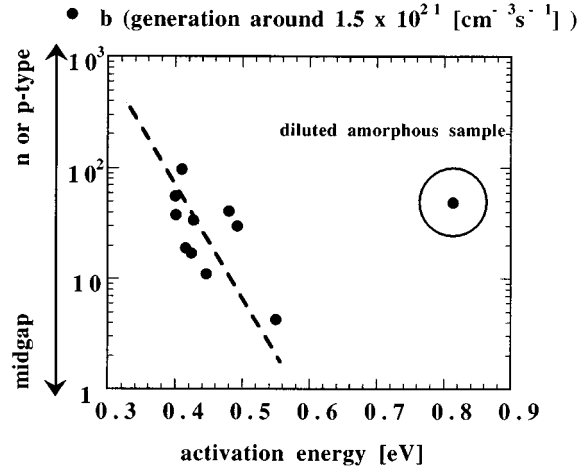


FIG. 6. Decrease of the parameter  $b$  as a function of the increase in the dark conductivity activation energy for  $\mu c\text{-Si:H}$  samples. The dashed line is only a guide to the eye.

deposited, at 110 MHz plasma excitation frequency, thereby studying the transition from microcrystalline to amorphous material. The dilutions were of 1.25%, 2.5%, 5%, and 7.6% of silane in hydrogen. The optical absorption spectrum shows the 7.6% sample to be amorphous and the 1.25% sample to be microcrystalline. Between these values the layers can be considered a mixture of amorphous and microcrystalline phase. It is clear from Figs. 7(a) and 7(b) that in this series, increasing crystalline volume fraction gives higher values for  $\sigma_{\text{photo}}$  and  $L_{\text{amb}}$ . For both  $L_{\text{amb}}$  and  $\sigma_{\text{photo}}$ , the values for microcrystalline samples are similar or enhanced (up to a factor 4 for the photoconductivity and up to factor 2 in ambipolar diffusion length) when compared to the amorphous sample of the series.

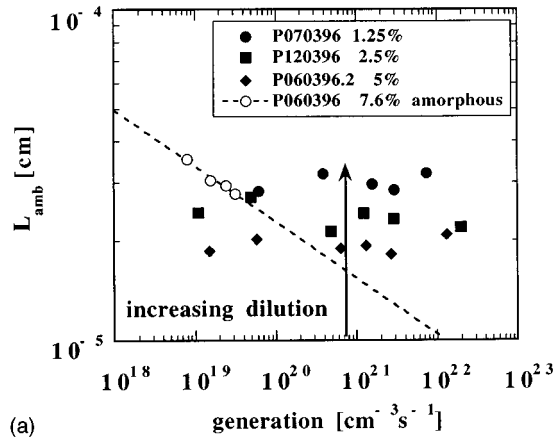
## CONCLUSIONS

Microcrystalline silicon is a promising new material for thin-film solar cells and other thin-film electronic devices, so its electronic properties are indeed of great interest. We show that, even if less easy to measure, both the photoconductivity and the ambipolar diffusion length in coplanar geometry can be determined. The values found in our  $\mu c\text{-Si:H}$  samples are of the same order or higher than in  $a\text{-Si:H}$ . In particular, for a dilution series of silane into hydrogen, we show that the microcrystalline sample prepared with the highest dilution has enhanced photoconductivity (up to a factor 4) and ambipolar diffusion length (factor 2) compared to the amorphous

TABLE I. Exponents of the power laws observed for the photoconductivity ( $\sigma_{\text{photo}} \propto G^\gamma$ ), the square of the ambipolar length ( $L_{\text{amb}}^2 \propto G^\lambda$ ), and for the parameter  $b$  ( $b \propto G^\theta$ ) as a function of the generation rate, for undoped amorphous silicon and for midgap microcrystalline silicon. The values for amorphous samples are those found for our ‘‘state of the art’’ samples (Ref. 12).

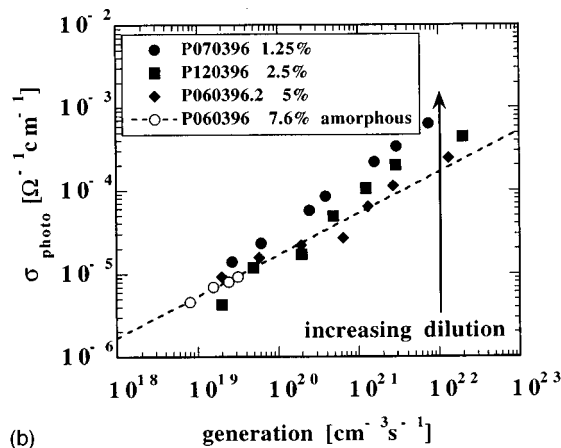
	Exponent of $\sigma_{\text{photo}}$ power law $\gamma$	Exponent of $L_{\text{amb}}^2$ power law $\lambda$	Exponent of $b$ power law $\theta$
Amorphous silicon samples	0.75 $\leftrightarrow$ 0.90	-0.50 $\leftrightarrow$ -0.10	-0.40 $\leftrightarrow$ 0.40
Microcrystalline silicon samples	0.50 $\leftrightarrow$ 0.85	-0.36 $\leftrightarrow$ 0.15	-0.55 $\leftrightarrow$ -0.10

dilation series 110 MHz



(a)

dilation series 110 MHz



(b)

FIG. 7. Effect of increasing the dilution from 7.6% to 1.25% of silane in total gas flow on the: (a) ambipolar diffusion length as a function of the generation rate and (b) photoconductivity as a function of the generation rate. Open circles are the values for the diluted amorphous sample measured only for low generation rates in order to avoid degradation. The dashed lines represent the power laws for this sample.

sample of the same series at high generation rates. Moreover, an increase in the values of both parameters is clearly correlated with the increase of dilution. It is clear that, due to the structural anisotropy of these  $\mu c$ -Si:H layers (growth is generally columnar<sup>2</sup>), measurements in “sandwich” configuration should be performed. As a first step, time-of-flight measurements have been carried out,<sup>20</sup> but to perform steady-

state measurements some other difficulties, such as ohmic contacts in the sandwich configuration (for SSPG or SSPC) or the influence of the Schottky barrier in the surface photovoltage method (SPV),<sup>21,22</sup> have to be resolved first. Meanwhile, reliable coplanar measurements still remain of great interest.

## ACKNOWLEDGMENT

This work was supported by the Swiss National Science Foundation under grants FN-39377 and FN-45696 and by the Swiss Federal Renewable Energy Program [EF-REN(93)032].

- <sup>1</sup>J. Meier, S. Dubail, R. Flückiger, D. Fischer, H. Keppner, and A. Shah, *Proceedings of the First WCPEC and by the Swiss Federal Renewable Energy Program* [EF-REN(93)032], Hawaii, 1994 (IEEE Inc., 1995), p. 409.
- <sup>2</sup>J. Meier, P. Torres, R. Platz, S. Dubail, U. Kroll, J. A. Anna Selvan, N. Pellaton Vaucher, C. Hof, D. Fischer, H. Keppner, A. Shah, K.-D. Ufert, P. Giannoulès, and J. Koehler, *Mater. Res. Soc. Symp. Proc.*, Vol. 420 (to be published).
- <sup>3</sup>N. Beck, J. Meier, J. Fric, Z. Remš, A. Poruba, R. Flückiger, J. Pohl, A. Shah, and M. Vaněček, *J. Non-Cryst. Solids* **198–200**, 903 (1996).
- <sup>4</sup>S. M. Cho, S. S. He, and G. Lucovsky, *Mater. Res. Soc. Symp. Proc.* **336**, 583 (1994).
- <sup>5</sup>F. Wang, R. Schwarz, S. Grebner, H. N. Liu, Y. L. He, and C. Z. Yin, *Proceedings of the 21st ICPS, Beijing, 1992*, p. 2008.
- <sup>6</sup>I. Balberg, *Mater. Res. Soc. Symp. Proc.* **258**, 693 (1992).
- <sup>7</sup>D. Ritter, K. Weiser, and E. Zeldov, *J. Appl. Phys.* **62**, 4563 (1987).
- <sup>8</sup>S. M. Sze, *Physics of Semiconductor Devices*, 2nd ed., published by Mohinder Singh Sejwal (Wiley Eastern Limited, New Delhi, 1983), p. 31.
- <sup>9</sup>A. Shah, E. Sauvain, and J. Hubin, *J. Non-Cryst. Solids* **114**, 402 (1989).
- <sup>10</sup>P. Pipoz, E. Sauvain, J. Hubin, and A. Shah, *Mater. Res. Soc. Symp. Proc.* **258**, 777 (1992).
- <sup>11</sup>J. Hubin, A. V. Shah, E. Sauvain, and P. Pipoz, *J. Appl. Phys.* **78**, 6050 (1995).
- <sup>12</sup>E. Sauvain, Ph.D. thesis, Université de Neuchâtel, 1992.
- <sup>13</sup>H. Curtins, N. Wyrsh, M. Favre, and A. V. Shah, *Plasma Chem. Plasma Process.* **7**, 267 (1987).
- <sup>14</sup>J. Meier, R. Flückiger, H. Keppner, and A. Shah, *Appl. Phys. Lett.* **65**, 860 (1994).
- <sup>15</sup>P. Torres, J. Meier, R. Flückiger, U. Kroll, J. A. Anna Selvan, H. Keppner, A. Shah, S. D. Littellwood, I. E. Kelly, and P. Giannoulès, *Appl. Phys. Lett.* **69** (in press, 1996).
- <sup>16</sup>M. Haridim, K. Weiser, and H. Mell, *Philos. Mag. B* **67**, 171 (1993).
- <sup>17</sup>E. Sauvain, A. Shah, and J. Hubin, *Proceedings of the 21st IEEE Photovoltaic Specialists Conference*, Kissimmee, Florida, 1990 (IEEE), p. 1560.
- <sup>18</sup>N. Beck, A. Shah, and N. Wyrsh, *Proceedings of the First WCPEC*, Hawaii, 1994 (IEEE), p. 476.
- <sup>19</sup>R. Flückiger, J. Meier, M. Goetz, and A. Shah, *J. Appl. Phys.* **77**, 712 (1995).
- <sup>20</sup>N. Wyrsh, M. Goerlitzer, N. Beck, J. Meier, and A. Shah, *Mater. Res. Soc. Symp. Proc.*, Vol. 420 (to be published).
- <sup>21</sup>A. Goodman, *J. Appl. Phys.* **32**, 2550 (1961).
- <sup>22</sup>A. R. Moore, *J. Appl. Phys.* **54**, 222 (1983).